

## DLTS: A Promising Technique for Understanding the Physics and Engineering of the Point Defects in Si and III-V Alloys

Aurangzeb Khan<sup>1</sup>, and Masafumi Yamaguchi<sup>2</sup>

<sup>1</sup>Electrical Engineering, University of South Alabama, 307 university Blvd, Mobile, AL, 36688

<sup>2</sup>Toyota Technological Institute, Nagoya, Japan

### ABSTRACT

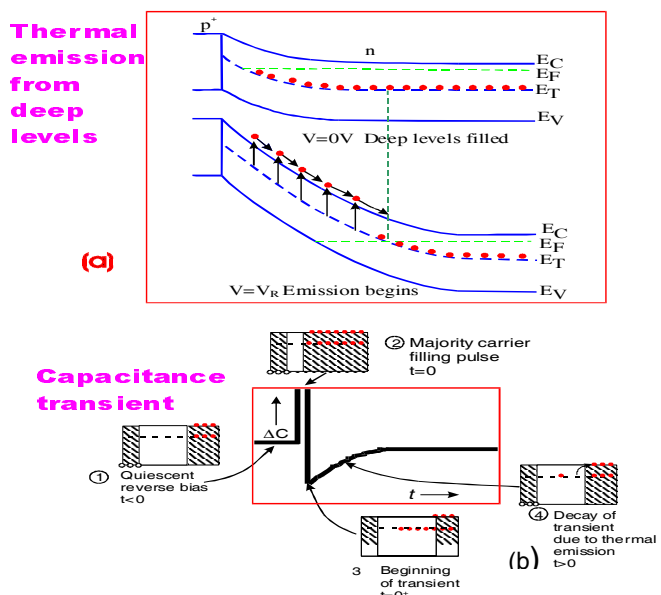
Deep level transient spectroscopy (DLTS) is the best technique for monitoring and characterizing deep levels introduced intentionally or occurring naturally in semiconductor materials and complete devices. DLTS has the advantage over all the techniques used to-date in that it fulfils almost all the requirements for a complete characterization of a deep centre and their correlation with the device properties. In particular the method can determine the activation energy of a deep level, its capture cross-section and concentration and can distinguish between traps and recombination centers.

In this invited paper we provide an overview of the extensive R & D work that has been carried out by the authors on the identification of the recombination and compensator centers in Si and III-V compound materials for space solar cells. In addition, we present an overview of key problems that remain in the understanding of the role of the point defects and their correlation with the solar cell parameters.

### INTRODUCTION

Deep Level Transient Spectroscopy (DLTS) is an efficient and powerful method used for observing and characterizing deep level impurities in semiconductors. The method was initially introduced by D. V. Lang [1] in 1974. DLTS is a capacitance transient thermal scanning technique, operating in the high frequency (Megahertz) range. It uses the capacitance of a p-n junction or Schottky barrier as a probe to monitor the changes in charge state of a deep centre. The capacitance techniques used prior to DLTS lacked either in sensitivity, speed, range of observable trap depths, or the spectroscopic nature, providing a limited characterization of a deep level.

Fig.1 Basic concept of thermal emission from a deep level and capacitance transient (a) energy band diagram of a p<sup>+</sup>n junction with an electron trap present at energy E<sub>T</sub> at zero applied bias and at steady reverse bias V<sub>R</sub>, (b) isothermal capacitance transient for thermal emission of the majority carrier traps. The condition for the trap occupation and free carrier concentration during various phases 1-4 of the transient are also shown. The un-shaded regions in the insets 1-4 show space charge width (after Lang [1]).



By contrast, DLTS fulfils almost all the requirements for a quick and complete characterization of a deep centre. DLTS is a technique, which is sensitive, rapid and easy to analyze. It is able to distinguish between majority- and minority-carrier traps [1]. DLTS can also give the concentrations, activation energy and capture cross-sections for both kinds of traps. It is spectroscopic in the sense that it can also resolve signals due to different traps. In the many variants of the basic DLTS technique the deep levels are filled with free carriers by electrical or optical methods. Subsequent thermal emission processes give rise to a capacitance transient. The transient is analyzed by signal processing while the temperature is varied at a constant rate. This results in a full spectroscopic analysis of electronic levels resident in the semiconductor band-gap.

For a complete understanding of DLTS we must have some basic knowledge of capacitance transients arising from the depletion region of a p-n junction. The use of capacitance transients for studying the properties of defect centers is well known. These transients provide information about an impurity level in the depletion region by observation of the capacitance transient originating from the return to thermal equilibrium after a perturbation is applied to the system. A brief description of the capacitance change due to the change in occupancy of the deep levels in the depletion region is given below.

When voltage across a p-n junction is changed, there is a corresponding change in the depletion region width (Fig.1). This change in width causes a change in the number of free charge carriers on both sides of the junction, resulting in a change in the capacitance. This change has two contributions; a) the contribution due to change in depletion width known as the junction capacitance and b) the contribution due to change in minority carrier concentration called the diffusion capacitance. Junction capacitance is dominant under reverse biased conditions while diffusion capacitance is dominant under forward biased conditions.

For a simple analysis of the response of the diode and interpretation of results, the junction is assumed to be asymmetric. An asymmetric diode is one in which one side of the junction is much more heavily doped than the other, implying that the space charge region is almost exclusively on the low doped side as shown in Fig. 1. Here we will consider a p<sup>+</sup>n diode with an electron emitting level. The depletion region is thus on the n-side.

The equation governing the capacitance transients of a p-n junction is given by,

$$C(t) = C_0 \left[ 1 - \frac{N_T}{2N_D} \exp\left(-\frac{t}{\tau}\right) \right] \quad (1)$$

where  $C_0$  is the capacitance at reverse bias,  $N_T$  the density of filled traps under steady state conditions,  $\tau$  is time constant, which gives emission rate, and  $N_D$  is the donor concentration. Thus the emission rates and trap concentrations can be determined from the changes in the capacitance of a p-n junction due to bias pulses. These changes are in the form of capacitance transients.

### Basic methodology of DLTS

The capacitance transients can be obtained by holding the sample at constant bias and temperature and applying a single filling pulse. The resultant isothermal transient can then be analyzed to obtain the emission rate of the carriers at that particular temperature. For obtaining a wide range of

emission rates, this is a time consuming technique. Also if many of deep levels are present, the experiment and its analysis become difficult. This is where DLTS has a major edge over the conventional techniques.

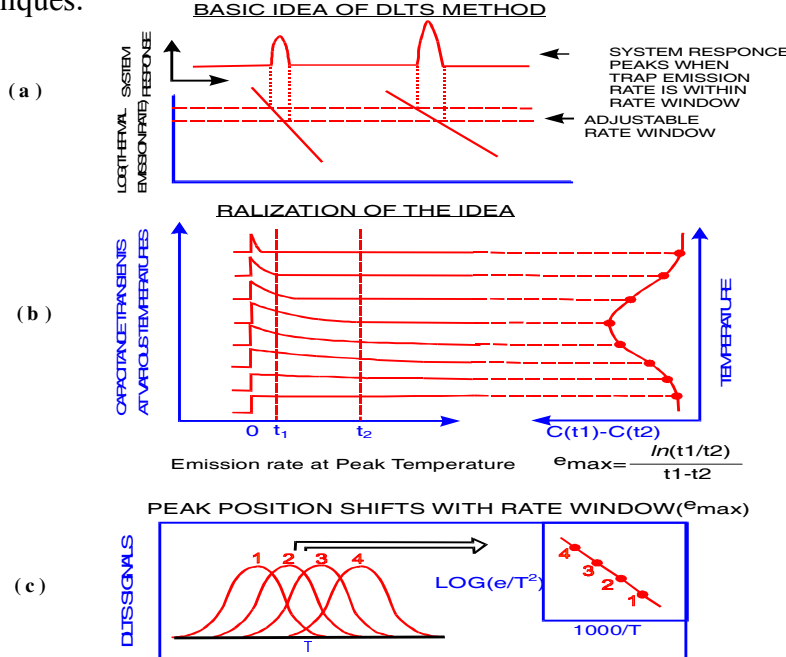


Fig. 2. Diagram illustrating the basic principles of DLTS (a) the rate window concept [after Lang], (b) application of the rate window concept using a time filter such as dual-gate box car shown here [after Lang[1]], (c) showing the shift of the peak positions in temperature with the rate window and the Arrhenius plot obtained from the peak positions.

The essential feature of DLTS [1] is its ability to set a *rate window* so that the measuring apparatus gives an output only when a transient occurs with a rate within the window. This concept is illustrated in Fig. 2. Thus if the sample temperature is varied at a constant rate, causing the emission rate of carriers from defect centre(s) present in it to vary, the measuring instrument will give a response peak whenever the defect centre emission rate is within the window. Instead of talking about rate window, we can say that the DLTS technique uses a time filter, which gives an output signal only when the transient has a time constant coinciding with the centre of the time window of the filter. A very important property of such a filter (time or rate) is that the output is proportional to the amplitude of the transient. Thus we can excite the diode repeatedly while the temperature is varied and by scanning over a large temperature interval we can directly get information as to which levels are present, their concentrations and by using different time/rate windows we can obtain the thermal activation energies of the levels.

## APPLICATIONS OF DLTS TECHNIQUE

### 1. Radiation-induced recombination centers in Si

In order to clarify the origins of radiation-induced defects in Si and correlation between their behavior and Si solar cell properties, DLTS analysis has been carried out. DLTS measurements were made using a quiescent bias of -2V and a saturating fill pulse of 2V, 1 ms duration.

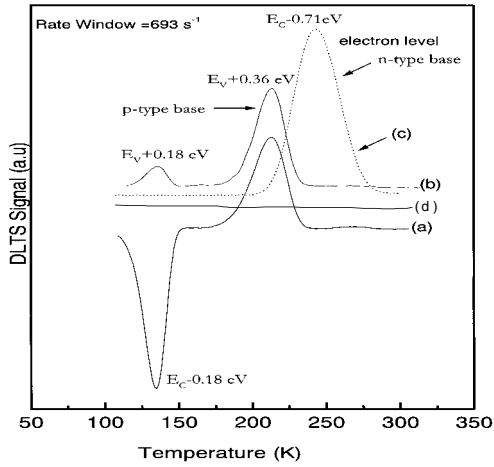


Fig. 3. DLTS spectra of p-type Si before and after 1 MeV electron irradiation: (d) before irradiation, (b) and (a) majority and minority carrier signals after  $1 \times 10^{16} \text{ cm}^{-2}$  fluence, respectively and (c) majority carrier signal after  $1 \times 10^{17} \text{ cm}^{-2}$  fluence. The base of the diode irradiated with  $1 \times 10^{17} \text{ cm}^{-2}$  electrons was n-type and required a correction to the spectrum to account for the effects of series resistance.

Fig. 3. shows both the majority- and minority-carrier DLTS spectra of some of the same Si diode as a function of 1 MeV electron fluence. A large concentration of a minority carrier trap with an activation energy of about  $E_C - 0.18 \text{ eV}$  has been observed, as well as the majority carrier traps at around  $E_v + 0.18 \text{ eV}$  and  $E_v + 0.36 \text{ eV}$ .

It is important to note that after annealing at  $250^\circ\text{C}$ , although the carrier concentration had recovered substantially, the observed concentration of the  $E_v + 0.36 \text{ eV}$  defects had increased as shown in the Fig. 4. This suggests that the  $E_v + 0.36 \text{ eV}$  defects are not principally responsible for carrier removal [2].

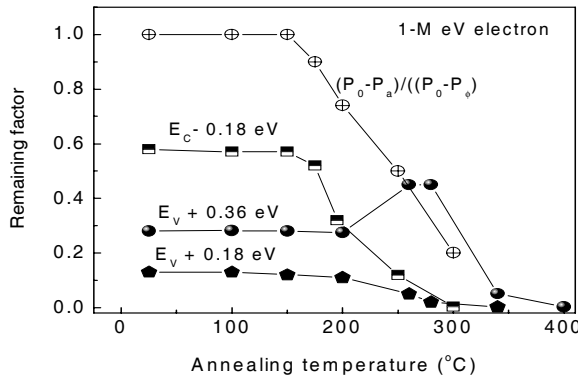


Fig. 4. Comparison of isochronal annealing of densities of  $E_c - 0.18 \text{ eV}$ ,  $E_v + 0.18 \text{ eV}$  and  $E_v + 0.36 \text{ eV}$  defect centers measured by DLTS with that of carrier concentration of p-type Si irradiated with 1-MeV electrons. Each annealing step duration was 20 min.[2]

We were able to confirm that the degradation of lifetime (diffusion length) is likely to be caused by the introduction of dominant hole level  $E_v+0.36\text{eV}$  and annealing behavior of this level govern the diffusion length recovery [2]. Fig. 5 compares isochronal annealing of density of the majority-carrier trap at  $E_v+0.36\text{eV}$  measured by DLTS and that of recombination center determined by solar cell properties in p-type Si irradiated with 1-MeV electrons. Changes in the relative recombination center density  $N_r$  with annealing were also estimated by changes in short-circuit current density  $J_{sc}$  of the solar cell according to the following equation:

$$\frac{N_{ra}}{N_{r\phi}} = \frac{\Delta(1/L_a^2)}{\Delta(1/L_\phi^2)} = \frac{[1/L_a^2 - 1/L_0^2]}{[1/L_\phi^2 - 1/L_0^2]} \sim \frac{\Delta(1/J_{sca}^2)}{\Delta(1/J_{sc\phi}^2)} = \frac{[1/J_{sca}^2 - 1/J_{sc\phi}^2]}{[1/J_{sc\phi}^2 - 1/J_{sc0}^2]} \quad (2)$$

Features of the  $E_v+0.36\text{eV}$  majority-carrier trap center with reverse annealing stage at  $200^0\text{C} \sim 300^0\text{C}$  and a recovery stage at around  $350^0\text{C}$  are similar to the changes in minority-carrier diffusion length  $L$  determined from the solar cell properties. This implies that the  $E_v+0.36\text{eV}$  majority-carrier trap center may also act as a recombination center.

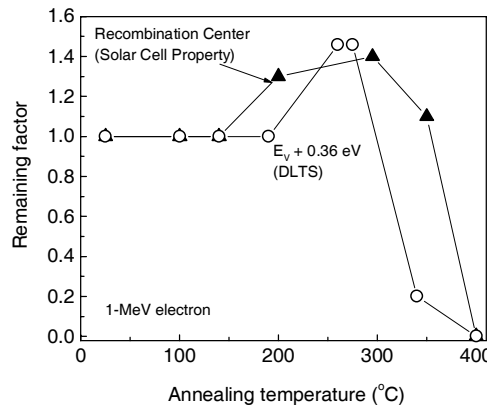
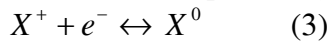


Fig. 5 Comparison of isochronal annealing of the majority-carrier trap at  $E_v+0.36\text{eV}$  measured by DLTS with that of the dominant recombination center determined by solar cell properties in p-type Si irradiated with 1-MeV electrons[2].

As shown in Fig. 4 the estimated initial concentration of the trap at approximately  $E_c-0.18\text{eV}$  is about 60% of the change in carrier concentration and therefore populous enough to be the dominating influence. Furthermore, the recovery of the carrier concentration after annealing occurs over roughly the same temperature range as disappearance of the minority trap signal. This evidence is, therefore, coherent with the hypothesis that the  $E_c-0.18\text{ eV}$  center is mainly responsible for the compensation of the base layer. The radiation-induced traps, which play an important role regarding the carrier removal and conduction type conversion of the base region, should be principally deep-level donors, which must be positively charged before electron capture.



## Role of Ga on compensator center

Interestingly, the introduction rate of the  $E_C$ -0.18 eV electron level in B-doped samples is strongly boron concentration dependent. Comparison of introduction behavior, annealing kinetics and the strong relation to boron and oxygen contents, supports correlation of this level ( $E_C$ -0.18 eV) with the  $B_i$ - $O_i$  (Fig. 6).

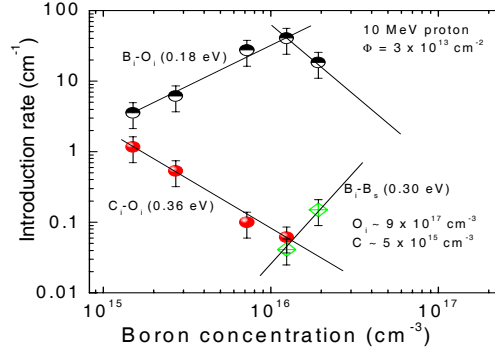


Fig. 6 Introduction rates of the interstitial related defects in 10 MeV proton irradiated p-Si as a function of background impurity concentration [3].

One of the most interesting and technological important feature of our work was the disappearance of the dominant donor like electron level  $E_C$ -0.18 eV in Ga-doped CZ- grown samples [4] (Fig. 7). As we have discussed above this level acts as a compensator center, which is positive charge before electron capture. The concentration of this level is about 60% of the change in carrier concentration after heavy fluences and therefore populous enough to be the dominating influence on device performance. This implies that carrier removal effects can be partially offset by using Ga as dopant instead of boron.

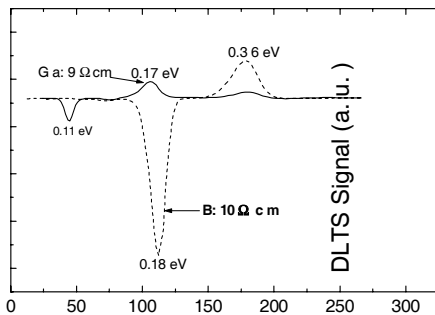


Fig. 7 Comparison of the minority carrier DLTS spectra measured for boron-or gallium -doped CZ-grown Si irradiated with 1-MeV  $3 \times 10^{16}$  electrons/ $\text{cm}^2$ . [4].

## SUPERIOR RADIATION RESISTANCE OF InGaP SOLAR CELLS

In this section, we present the direct observation of minority-carrier injection annealing of the dominant 1 MeV electron irradiation-induced hole trap labeled H2 located at 0.50-0.55 eV above the valence band in p-InGaP by Deep Level Transient Spectroscopy (DLTS). Furthermore, an evidence of a large minority carrier capture cross section for this hole trap has been obtained by

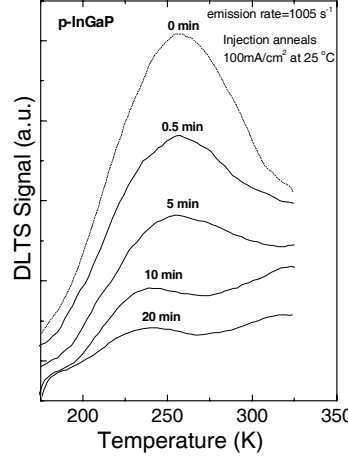


Fig. 8. Changes of the DLTS spectrum of trap H2 with various time of injection at 25°C with an injection density of  $0.1 \text{ A cm}^{-2}$  [5].

double-carrier pulse DLTS which demonstrate the important role of this trap as an recombination center. The one aim of present study was to clarify the mechanism involved in minority-carrier injection-enhanced annealing of the radiation-induced defect H2 in p-InGaP [6-11].

The important result of this study is the influence of minority-carrier injection on the annealing kinetics of dominant hole level H2 [5]. In order to clarify the recovery of the solar cells properties following minority-carrier injection annealing, we carried out a systematic study of the variation of the concentration of the hole level H2 using a constant amplitude of forward bias injection ( $0.1 \text{ A/cm}^2$ ) at various temperatures for 0.5, 1, 2, 5, 10 and 20 min. The majority-carrier emission DLTS scans taken after different forward bias injection steps show a pronounced reduction in the H2 amplitude as shown in Fig. 8, which is correlated with a recovery of the maximum power output of the solar cells. It should be noted that the H2 peak; is rather broad and after pronounced reduction following forward bias, exhibits a double structure, indicating that this peak consists of more than one closely spaced peaks; one on the high temperature side appear to anneal relatively slowly

Figure 9 presents the temperature dependence of the annealing rate  $A^*$  of the hole trap H2 by minority-carrier injection-enhanced processes, determined from DLTS. A comparison is given with the injection-enhanced annealing rates estimated by changes in short-circuit current density  $J_{sc}$  of the solar cells according to the following:

$$\frac{N_{T\phi}}{N_{T\phi}} = \frac{L_\phi^2 (L_0^2 - L_I^2)}{[L_I^2 (L_0^2 - L_\phi^2)]} \sim \frac{J_{sc\phi}^2 (J_{sc0}^2 - J_{scI}^2)}{[J_{scI}^2 (J_{sc0}^2 - J_{sc\phi}^2)]} \quad (4)$$

where suffixes 0,  $\phi$ , and I correspond to before and after irradiation, and after injection, respectively. The important result of this study is the direct relationship between the annealing rates, the solar cells properties and the H2 trap.

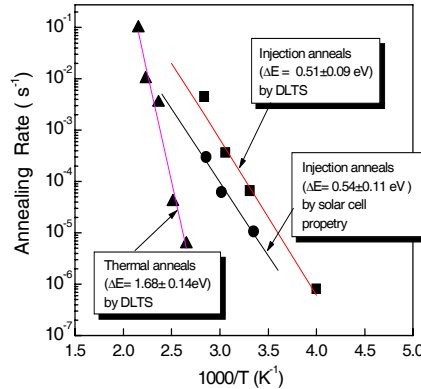


Fig. 9. Temperature dependence of the thermal and injection annealing rates of the radiation-induced defects in p-InGaP, determined from solar cells property ( $J_{sc}$  or  $L$ ) and for H<sub>2</sub> trap observed by DLTS [5].

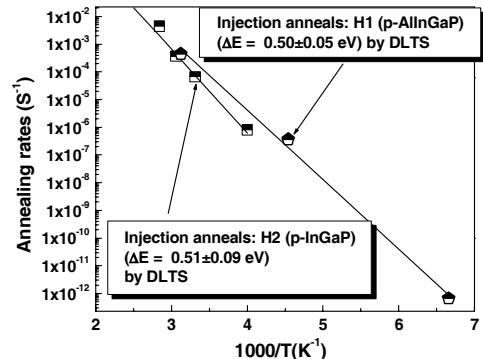
A close agreement between activation energy for recovery of radiation-induced defects, determined by solar cell properties and for the hole traps H<sub>2</sub>, demonstrates that this trap controls the minority-carrier lifetime. This result demonstrates that the dominant majority hole level H<sub>2</sub> ( $E_V + 0.5 - 0.55$  eV) is the recombination center, which governs the minority-carrier lifetime in n<sup>+</sup>-p InGaP solar cells.

## SUPERIOR RADIATION RESISTANCE OF AlInGaP SOLAR CELLS

Figure 10 presents the temperature dependence of the annealing rate  $A$  of the trap H<sub>1</sub>, in p-AlInGaP determined by DLTS. The annealing activation energy of electron irradiation-induced defect H<sub>1</sub> in p-AlInGaP is evaluated to be 0.50 eV. A comparison is provided with the injection-enhanced annealing rates estimated for the defect H<sub>2</sub> in p-InGaP. It is to be noted that the minority carrier injection annealing properties of the defect H<sub>2</sub> in p-InGaP observed in the previous 1 MeV electron study are almost the same as those observed in the present study of H<sub>1</sub> defect in p-AlInGaP after 1 MeV electron irradiation, which identified that the defect H<sub>1</sub> observed in p-AlInGaP has the same nature of the defect H<sub>2</sub> previously observed in P-InGaP and H<sub>4</sub> in InP [12,13].

The recovery of the radiation damage due to minority carrier injection under forward bias is thought to be caused by an energy release mechanism in which enhancement is induced by the energy released when a minority carrier is trapped on the defect site. According to this mechanism, a change of charge states due to capture of carriers can result in electron phonon coupling. That is, vibration relaxation occurs, which may activate various reactions of the defect such as its migration or destruction, and ultimately decays to heat the lattice. The detailed analysis of this mechanism was previously studied in case of defects in InP, GaAs, and InGaP by the authors and others.

Fig. 10. Comparison of the temperature dependence of injection annealing rates of the radiation-induced defect H<sub>1</sub> ( $E_V + 0.37$  eV) in p-AlInGaP and H<sub>2</sub> ( $E_V + 0.55$  eV) in p-InGaP [13].



In summary, DLTS is an effective spectroscopy technique for processing transient (capacitance or current) from deep levels. This technique has proved to be an instrumental in determining most of the properties of the defects such as structure, introduction rates, introduction mechanism, thermal stability of the defects etc. DLTS is particularly attractive because it can be used to characterize defects using various kinds of space charge based devices such as Schottky barrier diodes, and p-n junction to quantum well based complex devices. In addition, sensitivity of the DLTS for detecting defects in concentration of  $10^9 \text{ cm}^{-3}$  is superior to any other characterization technique. In this paper we have reviewed the extensive work, on the electronic properties of the recombination and compensator centers in Si and III-V compound materials for space solar cells.

## REFERENCES

1. D. V. Lang, J. Appl. Phys. 45, 3023 (1974).
2. M. Yamaguchi, A. Khan, S. J. Taylor, K. Ando, T. Yamaguchi, S. Matsuda, and T. Aburaya, J. Appl. Phys. 86, 217 (1999).
3. A. Khan, M. Yamaguchi, M. Kaneiwa, T. Saga T. Abe, O. Annzawa and S. Matsuda. J. Appl. Phys. 90, 1170(2001).
4. A. Khan, M. Yamaguchi, M. Kaneiwa, T. Saga T. Abe, O. Annzawa and S. Matsuda. J. Appl. Phys. 87, 8389 (2000).
5. A. Khan, M. Yamaguchi, J.C. Bourgoin and T. Takamoto., Appl. Phys. Lett. 76, 2550 (2000).
6. J. C. Bourgoin and J. W. Corbett, Radiation Effects 36, 157 (1978).
7. L. C. Kimerling, Solid State Electronics, 21, 1391 (1978).
8. L. C. Kimerling and D. V. Lang, Inst. Phys. Conf. Ser. 23, 589 (1975).
9. J. C. Bourgoin and J. W. Corbett, Phys. Lett. 83A, 135 (1972).
10. J. C. Bourgoin and J. W. Corbett, Inst. Phys. Conf. Ser. 23, 149 (1975).
11. D. V. Lang and L. C. Kimerling, Phys. Rev. Lett. 35, 22 (1975).
12. A. Khan, Masafumi Yamaguchi, Jacques C. Bourgoin, and Tatsuya Takamoto. J. Appl. Phys. 89, 4263 (2001).
13. A. Khan, S. Marupaduga , M. Alam, N. J. Ekins-Daukes, Appl. Phys. Lett. 85, 5218 (2004).